Effect of disorder produced by cationic vacancies at the *B* sites on the electronic properties of mixed valence manganites

J. Vergara, R. J. Ortega-Hertogs, and V. Madurga
Departamento de Física, Universidad Pública de Navarra, E-31006 Pamplona, Spain

F. Sapiña, Z. El-Fadli,* E. Martínez, and A. Beltrán
Institut de Ciència dels Materials de la Universitat de València, E-46100 Burjassot, Spain

K. V. Rao
Department of Condensed Matter Physics, The Royal Institute of Technology, S-10044 Stockholm, Sweden
(Received 14 October 1998; revised manuscript received 4 February 1999)

An alloy series of single-phased polycrystalline $La_{1-x}Na_xMnO_{3+\delta}$ ($0 \leqslant x \leqslant 0.15$) has been synthesized in order to study the effect of disorder on the electronic properties of mixed valence manganites. The synthetic variables allow one to maintain a constant proportion of Mn^{4+} in the samples ($Mn^{3+}/Mn^{4+} = 2.1 \pm 0.2$), while the similar size of La^{3+} and Na^{+} ions results in no appreciable change in the tolerance factor of the perovskite structure throughout the series. In this way, the sodium content x controls the concentration of cationic vacancies at the B (Mn) sites. The presence of these vacancies gives rise to a change in the periodic potential at the Mn sites adjacent to such vacancies, thus influencing the electronic band structure of these materials. All the samples undergo a ferro- to paramagnetic transition, at temperatures that vary from 330 to 140 K as the disorder increases. Concomitantly, the residual resistivity in the low-temperature metalliclike regime increases by eight orders of magnitude. The $x = 0.00$ sample, i.e., the sample having the largest concentration of vacancies in the series, presents a distinctive behavior: it shows semiconductorlike resistivity and a magnetic behavior reflecting an inhomogeneous magnetic state. These results have been explained on the basis of the effect of structural disorder on the electronic band structure. Above the transition temperature, thermopower and resistivity measurements suggest a polaronic character of the conductivity. Polaron formation energies ($\approx$200 meV) are found to be nearly independent of the degree of disorder in the samples. Our results suggest that metallic ferromagnetic regions and semiconducting cluster-glass zones coexist below T_c. With increasing disorder, the semiconducting regions grow in volume, which modifies the transport and magnetotransport properties of these samples. [S0163-1829(99)12325-7]

I. INTRODUCTION

Although mixed valence manganites have been studied for more than 40 years,[1–3] the recent discovery of colossal magnetoresistance (CMR) in these materials has renewed the interest in them.[4,5] Thus, apart from technological applications,[6] further detailed studies of these materials have become relevant in order to understand the underlying mechanisms that give rise to the observed large magnetoresistance. Ferromagnetism in these systems has been usually explained in terms of the double-exchange (DE) mechanism proposed by Zener:[1] the e_g antibonding electrons can hop between neighboring Mn ions when these are ferromagnetically coupled. Thus, electron hopping produces metalliclike conductivity as well as the ferromagnetism in mixed-valence manganites, such as $La_{1-x}Ca_xMnO_3$, whereas the parent compounds $LaMnO_3$ and $CaMnO_3$ are antiferromagnetic insulators. Actually, the DE mechanism allows us to explain the change in resistivity associated with the para- to ferromagnetic transition: the ordered arrangement of spins enables electron hopping between neighboring Mn atoms in the low-temperature phase but spin disorder prevents such hopping processes in the high-temperature phase. However, the change of resistivity is too large to be ascribed solely to the DE mechanism.[7] Localization of the charge carriers as magnetic polarons (due to strong electron-phonon coupling, associated presumably to the Jahn-Teller effect) is very likely the key factor to explain the observed huge values of the magnetoresistance.[8,9]

Systematic explorations of mixed-valence alkaline-earth lanthanide manganites have shown the relevance for CMR of the mean oxidation state of the manganese ions, with an optimum value close to 3.33.[10] These studies also indicate the existence of a certain relationship between the transition temperature and the tolerance factor t of the perovskite structure ABO_3, which is a measure of the mismatch between the equilibrium A-O and Mn-O bond lengths.[11] The t value determines in practice the structural distortion of the perovskite structure, that is, the Mn-O-Mn angle, and hence the transfer integral t_σ^F between Mn^{3+} and Mn^{4+} ions.

Despite the above, our results in the study of the $La_{1-x}K_xMnO_{3+\delta}$ system have shown that the values of the Mn^{4+} concentration c and the tolerance factor (or the mean size of cations at A sites, $\langle r_A \rangle$) are not able to characterize by themselves the electronic behavior of these materials.[12] Therefore, in order to characterize completely these compounds, we proposed the use of a new parameter: the concentration of vacancies at the B perovskite sites v_B. In fact, preliminary results of the electronic characterization of the

TABLE I. Selected chemical, structural, magnetic, and transport parameters of the samples of the series $La_{1-x}Na_xMnO_{3+\delta}$. The meaning of each symbol is explained in the text.

x	Stoichiometry	% Mn^{4+}	v_B (%)	t	T_c (K)	T_R (meV)	E_ρ (meV)	E_S (meV)	W_H (meV)	$\mu_{\text{eff}}^{\text{th}}$ (μ_B)	$\mu_{\text{eff}}^{\text{CW}}$ (μ_B)	μ^M (μ_B)	μ^{th} (μ_B)	Magnetic structure
0.0	$La_{0.949}Mn_{0.949}O_3$	35	5.1	0.994	145		127	15	112	4.4	5.9	3.1	3.5	Non collin.
0.03	$La_{0.929}Na_{0.029}M_{0.958}O_3$	30	4.2	0.993	175	110	137	15	122	4.4	5.1	3.6	3.55	Ferro
0.06	$La_{0.910}Na_{0.058}Mn_{0.968}O_3$	31	3.2	0.993	245	200	150	8	142	4.5	4.9	3.7	3.6	Ferro
0.09	$La_{0.889}Na_{0.088}Mn_{0.977}O_3$	35	2.3	0.993	290	250	132			4.5	4.9	3.65	3.6	Ferro
0.12	$La_{0.866}Na_{0.118}Mn_{0.984}O_3$	33	1.6	0.994	315	275	102			4.6	5.0	3.7	3.65	Ferro
0.15	$La_{0.844}Na_{0.149}Mn_{0.993}O_3$	31	0.7	0.994	330	290	90			4.7	5.3	3.7	3.7	Ferro

$La_{1-x}Na_xMnO_{3+\delta}$ system have allowed us to determine relevant points in the electronic phase diagram of this system. Together with those previously obtained in the case of the $La_{1-x}K_xMnO_{3+\delta}$ system, they have revealed the existence of a correlation between the critical temperature for ferromagnetic ordering and the concentration of vacancies at the B sites, in samples with a fixed concentration of Mn^{4+} (close to the optimal).[13]

In this work we present a comprehensive study of how the electric and magnetic properties of $La_{1-x}Na_xMnO_{3+\delta}$ samples are modified by the presence of vacancies at the B sites. In practice, our contribution is in debt to earlier data and interpretations referred, in general, to the influence of defects on the electronic properties of mixed valence manganites. In previous studies on the system $LaMnO_{3+\delta}$, the influence of the concentration of vacancies, the concentration of Mn^{4+} and the tolerance factor of the perovskite structure have been considered.[14] However, as far as usually several of these factors are simultaneously modified, it results intricate to weigh up the role of each variable on the identified tendencies. In the present study, the concentration of Mn^{4+} and the tolerance factor are kept practically constant through the entire manganite series. Hence, the effect of the vacancies can clearly be shown.

II. EXPERIMENT

Polycrystalline $La_{1-x}Na_xMnO_{3+\delta}$ samples, where $x = 0.00$, 0.03, 0.06, 0.09, 0.12, and 0.15, were prepared by thermal decomposition of precursors obtained by freeze drying of acetic acid solutions of the appropriate salts of the metals in the required stoichiometric ratios. A detailed description of the preparation and characterization of the samples is given elsewhere.[13] Further lanthanum substitution can give rise to secondary phases, as in the potassium series.[12] The use of this precursor-based synthetic method has allowed us to synthesize single-phased perovskites at low temperatures. The incorporation of sodium in the perovskite lattice at low temperature avoids its subsequent evaporation, and makes possible, in contrast to the ceramic procedure, a reliable control of the stoichiometry. The stoichiometry and mean oxidation state of the manganese ions are given in Table I.

ac susceptibility measurements have been carried out in a homemade ac susceptometer, in the temperature range 80–345 K, at a magnetic-field amplitude of 1 Oe and a frequency of 181 Hz. Magnetic measurements (temperature dependence of magnetization in high and low fields) were performed in a Quantum Design superconducting quantum interference device magnetometer, over the temperature range 5–350 K, in magnetic fields up to 10 kOe. Additional magnetization measurements have been carried out in an EG&G vibrating sample magnetometer up to 500 K.

dc resistivity and magnetoresistivity measurements were made on sintered pellets using the standard four-probe technique in the temperature range 5–350 K, in magnetic fields up to 10 kOe. Thermopower measurements were made locating the samples in a temperature gradient of ~10 K, and changing the temperature from 75 to 290 K. The magnetic field was varied between 0 and 10 kOe. All the thermoelectric data are evaluated relative to the thermoelectric power of Cu.

III. RESULTS

A. Magnetic properties

The measured temperature dependence of the magnetic moment of the samples is shown in Fig. 1. The applied magnetic field in all these measurements was 9 kOe. In this field, technical saturation was reached for all the samples. A transition from a low-temperature ferromagnetic phase to a high-temperature paramagnetic phase is evident. The transition temperature T_c increases with x (i.e., when the structural disorder decreases, as discussed later). However, not only the magnetic transition temperature is modified by the disorder but also the net magnetic moment per Mn atom and the low-temperature dependence of the magnetic moment. For instance, the experimental value of the magnetic moment at 10 K, μ^M, for the $x=0.00$ sample (the one with higher disorder) is 12% smaller than the theoretical one μ^{th}, which has been calculated assuming that the magnetic moment of the Mn^{3+} is $4\mu_B$ and the one of the Mn^{4+} is $3\mu_B$ (see Table I). Also, for the $x=0.00$ sample, the value of the magnetization continuously increases as the temperature is decreased to 10

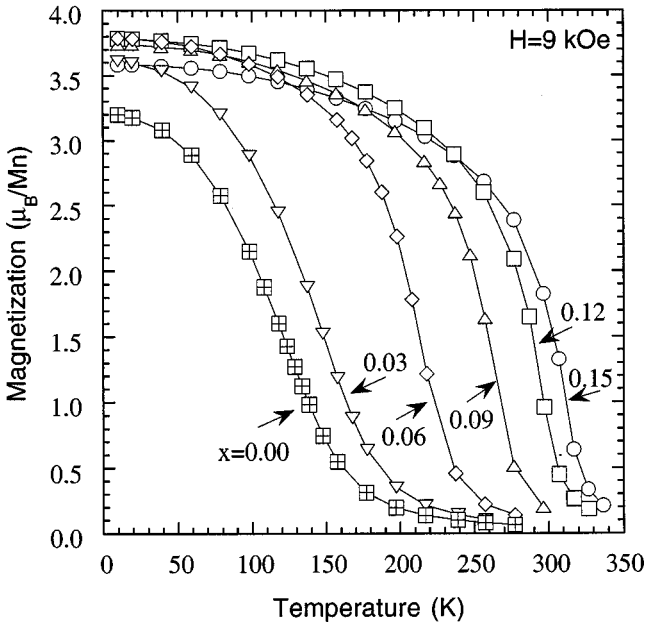

FIG. 1. Thermal variation of the magnetization at an applied field of 9 kOe for $La_{1-x}Na_xMnO_{3+\delta}$.

K, meanwhile the samples with $x \geq 0.06$ exhibit an almost temperature-independent behavior in the low-temperature range.

Zero-field-cooled (ZFC) and field-cooled (FC) runs show also special features in the magnetization of the samples with lower Na content, cf. Fig. 2. The initial rise of the magnetization of the samples $x=0.00$ and $x=0.03$ in the ZFC experiments suggests the presence of competing exchange interactions (the superexchange antiferromagnetic t^3-p_π-t^3 interaction and the ferromagnetic double exchange e^1-p_σ-e^0 one).[19] The remaining samples in the series ($x \geq 0.06$) do not exhibit this particular characteristic, which suggests that the ferromagnetic interaction dominates in these samples.

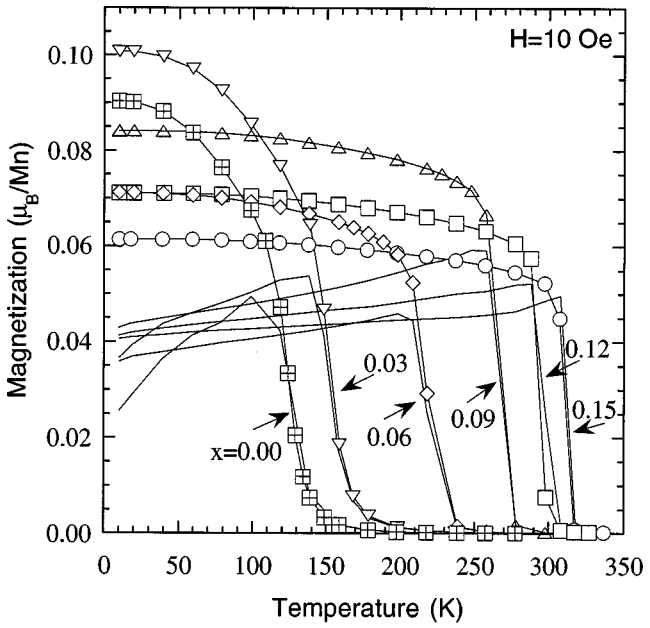

FIG. 2. Zero-field-cooled (ZFC), continuous lines, and field-cooled (FC), symbols, magnetization warming runs at an applied field of 10 Oe. Temperature range 10–300 K.

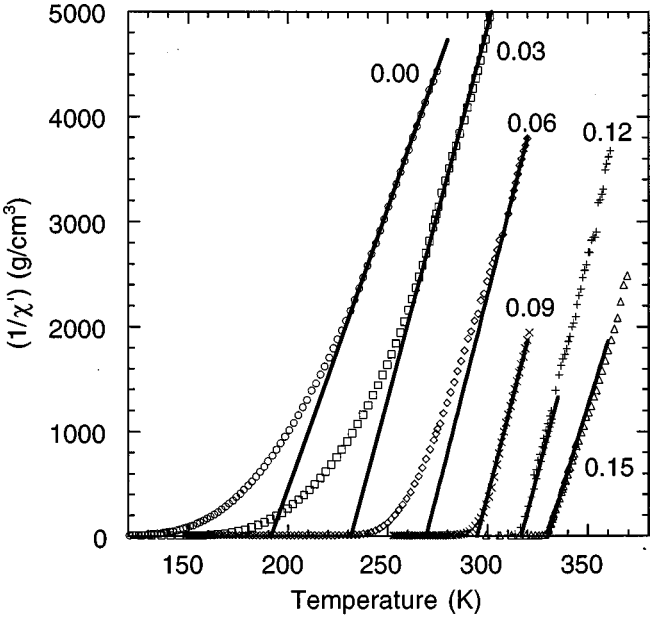

FIG. 3. Thermal variation of the inverse of the in-phase component of the ac susceptibility $\chi'(T)$. Solid lines represent the fit to the Curie-Weiss law.

In Fig. 3 the temperature dependence of the inverse of χ' is presented. The obtained effective magnetic moment values $\mu_{\text{eff}}^{\text{CW}}$, are found to be considerably larger than the theoretical ones, $\mu_{\text{eff}}^{\text{th}} = g\sqrt{J(J+1)}\mu_B$. In this formula the value of the Landé factor g has been taken as 2. Also $J=S$ since the orbital angular momentum is quenched by the crystalline field. The values of the spin quantum number S of the Mn^{3+} and Mn^{4+} ions are, respectively, 2 and 3/2, within a model of localized electrons. μ_B is the Bohr magneton. This result indicates that a purely paramagnetic regime has not been reached. In addition, there exists a wide temperature range above T_c where stronger short-range ferromagnetic interactions are present, as evidenced by the significant differences between the paramagnetic and ferromagnetic Curie temperatures. In fact, this difference, which approximately increases as the structural disorder does, becomes as high as 90 K ($x = 0.03$), whereas it does not exceed 30 K around in a typical ferro- to paramagnetic transition.

B. Transport properties

Figure 4 shows the temperature dependence of the resistivity at zero field. The samples $x \geq 0.03$ exhibit upon cooling a clear transition from insulator ($\partial\rho/\partial T < 0$) to metalliclike behavior ($\partial\rho/\partial T > 0$). Thus, a maximum in the resistivity, characteristic of the semiconductor-to-metal transition, is observed at a temperature T_R, slightly below the magnetic transition temperature, which is a feature of structurally disordered mixed-valence manganites.[16] The observed T_R values for our samples are listed in Table I. In contrast, the $x = 0.00$ sample shows semiconductorlike behavior in the whole temperature range, although it exhibits a magnetic phase transition to a ferromagnetic state. This result, which is fairly surprising (since ferromagnetism and metallic conduc-

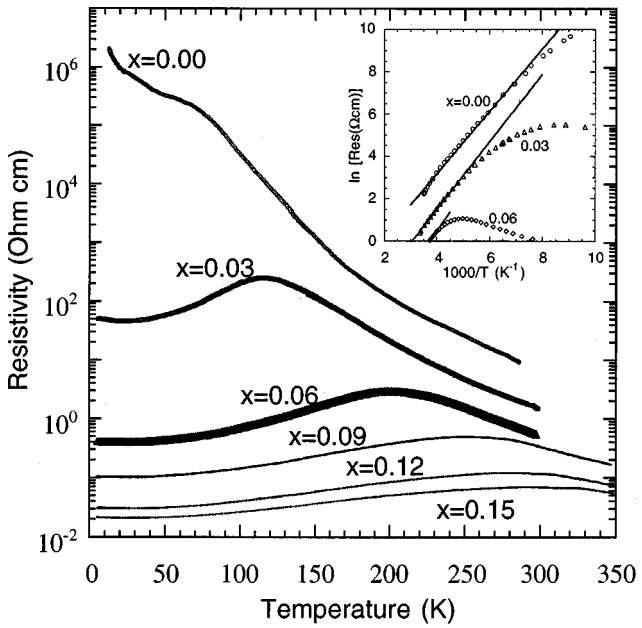

FIG. 4. Thermal variation of the zero-field resistivity for $La_{1-x}Na_xMnO_{3+\delta}$. The inset represents the fit of the resistivity to a small polaron behavior in the adiabatic limit, as indicated in the text. Parameters values are listed in Table I.

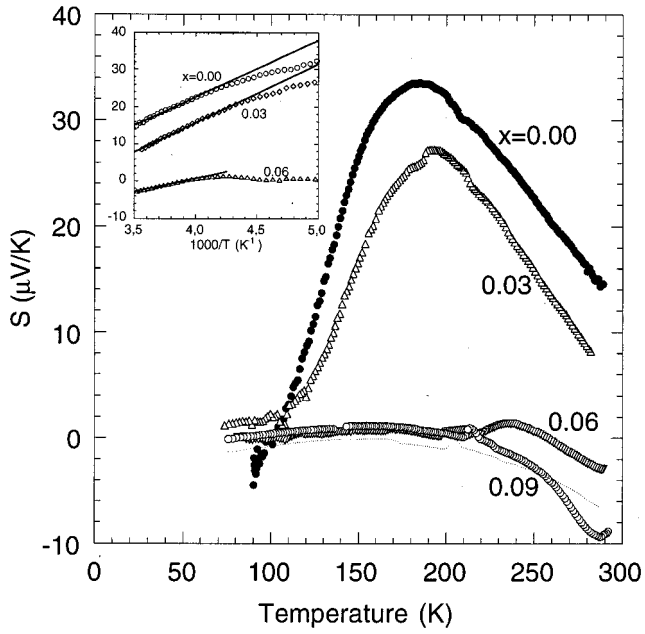

FIG. 6. Thermal variation of the zero-field thermopower for the samples $x \leqslant 0.09$. The inset displays the fit of the thermopower to a small polaron behavior in the adiabatic limit, as indicated in the text. Parameters values listed in Table I.

tivity usually appear as directly related through the DE mechanism), will be explained below in terms of the structural disorder in this sample.

The application of a magnetic field reduces significantly the resistivity below the transition temperature. The magnetoresistance MR is defined as $[\rho(0,T)-\rho(H,T)]/\rho(0,T)$. The sample $x=0.03$ shows the maximum effect. It reaches a value of 37% in a magnetic field of 1 T. In Fig. 5, the thermal variation of the MR is represented. The temperature dependence of the MR for our samples can be explained on the basis of two different mechanisms.[17,18] One of them is the spin tunneling across the grain boundaries.[17] This contribution is more significant at low temperature and low magnetic fields. It produces a continuous increase of the MR values as the temperature is lowered. The other contribution comes from the suppression of magnetic fluctuations as the field is increased. This process takes place within the volume of the grains. This one is dominant in the vicinity of the magnetic transition temperature and is not saturated even in magnetic fields of the order of 10 T.[18] Since the grain size in our samples is roughly constant $\approx$200 nm, surface and volume effects need to be taken into account when studying the MR. Also, the applied magnetic fields, $H=10$ kOe, are relatively small. In this particular situation, both mechanisms, spin tunneling and the suppression of magnetic fluctuations, seem to compete with similar strengths, thus originating the presence of a peak or an inflection near the temperature of the resistivity maximum T_R, cf. Fig. 5.

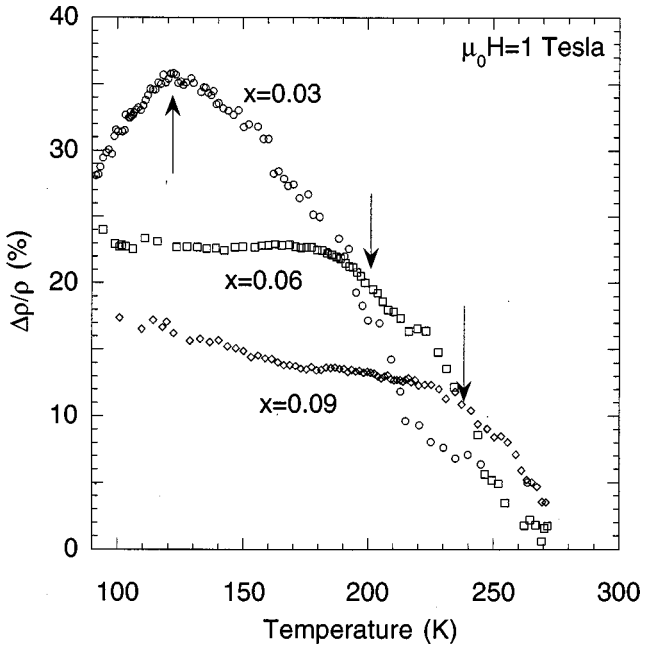

FIG. 5. Thermal variation of the magnetoresistance in an applied field of 10 kOe for the samples that show the highest values. The arrows indicate the temperature of the resistivity peak.

Measurements of the thermoelectric power $\alpha(T)$ as a function of the temperature in the range 77–300 K are shown in Fig. 6. On cooling down from 300 K, the absolute value of $\alpha(T)$ increases. As the transition temperature (T_c) is reached, the transport behavior of the samples is modified: the carriers start to delocalize (as corresponds to a metallic behavior) and, subsequently the absolute value of thermoelectric power decreases. But as already pointed out in the description of the magnetic measurements (cf. Figs. 1 and 2), the samples $x=0.00$ and 0.03 show a different behavior when compared with those for the other samples in the series. Although all of them exhibit a relative maximum in the absolute value of the Seebeck coefficient S, cf. Fig. 6, at a temperature close to T_c, the $x=0.00$ and $x=0.03$ samples show significantly higher values of $\alpha(T)$ around the transi-

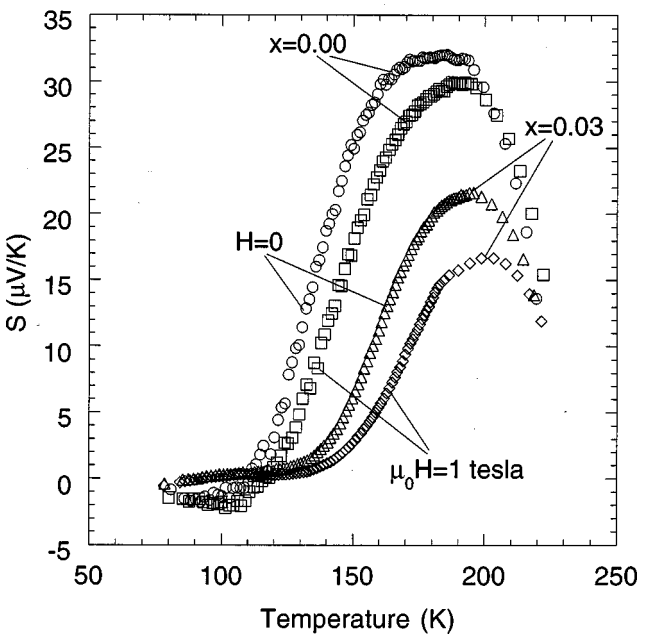

FIG. 7. Thermal variation of the thermopower $\alpha(T,H)$ at applied fields of 0 and 10 kOe for the samples $x=0.00$ and $x=0.03$.

tion temperature. This is an indication of their strong semiconducting character. We will return to this subject later on.

The effect of the magnetic field on the thermoelectric power of the sample $x=0.03$ is shown in Fig. 7. The application of a magnetic field produces a displacement to higher temperatures of the maximum and a reduction in this value. A spin entropy term is thus contributing significantly to the thermoelectric power of the samples $x=0.00$ and $x=0.03$, which are the ones that experience the highest reductions in their Seebeck coefficients.

IV. DISCUSSION

A. Effect of cationic vacancies

It is well established that the structure and behavior of the perovskites ABO_3 are determined by the relative equilibrium between the A-O and B-O bond lengths, characterized by the tolerance factor, defined as

$$t=\frac{A-\mathrm{O}}{\sqrt{2}B-\mathrm{O}},$$

where A-O and B-O are the distances between the oxygen and the cations at A and B sites, respectively, of the perovskite structure.[19] For $t<1$, the B-O bonds are under compression and the A-O bonds are under tension. In order to mitigate these stresses, a cooperative rotation of the BO_6 octahedra about an axis of the ideal cubic structure occurs. This rotation bends the B-O-B bond angle from 180° to 180-ϕ°, and ϕ increases as t decreases. In the case of the manganese perovskites, this structural stress can also be lessened by oxidation of the MnO_3 array. By removing antibonding electrons, the mean equilibrium Mn-O bond length becomes shortened, which results in a t value closer to 1. In samples prepared at high oxygen activities, as is the case of the samples studied in this work $[\ln a(\mathrm{O}_2)=0]$, an oxygen excess is normally observed in the structure.[20] However, there are no interstitial sites in the perovskite structure for this oxygen excess, and hence, the nonstoichiometry δ is accommodated as cation vacancies. In consequence, from the structural point of view, the correct notation of the perovskites studied in this work should be

$$(\mathrm{La}_{1-x}\mathrm{Na}_x)_{3/(3+\delta)}(\mathrm{V_{La}})_{\delta/(3+\delta)}(\mathrm{Mn})_{3/(3+\delta)}(\mathrm{V_{Mn}})_{\delta/(3+\delta)}\mathrm{O}_3$$

for a $(La_{1-x}Na_x)$:Mn ratio 1:1. The results of the chemical analyses of these compounds, listed in Table I, indicate that the deviation from this ratio is negligible and, thus, the concentration of cationic vacancies at A and B sites, V_{La} and V_{Mn} respectively, is the same for a given sample of the series.[13] This concentration is listed in Table I under the column v_B.

Another interesting fact is that the concentration of Mn^{4+} remains practically constant $(c=33\pm2\%)$ for all the compounds studied in this work, cf. Table I. We have previously obtained the same result in our study of the $La_{1-x}K_xMnO_{3+\delta}$ system. Other authors have obtained similar results in the $La_{1-x}Sr_xMnO_{3+\delta}$ system, working at oxygen activities and temperatures close to the ones used in our studies.[20] As far as the mean oxidation state of manganese ions is practically constant throughout the series, the sodium content controls the concentration of cationic vacancies in the $Mn_{1-\varepsilon}O_3$ array; $\varepsilon[\varepsilon=\delta/(3+\delta)]$ decreases with the increase in x, as listed in Table I. On the other hand, as far as the Na^+ ions are only slightly larger than the La^{3+} ones, the variation of the tolerance factor t is not significant, cf. Table I. These facts make possible to clearly observe systematic tendencies due to the variation of the concentration of vacancies in this system.

Particularly in our samples, it has been mentioned that both the total concentration of holes and the tolerance factor of the perovskite structure do not vary considerably through the $La_{1-x}Na_xMnO_{3+\delta}$ series, although the structural disorder increases contrary to x, being maximum for the $x=0.00$ sample. It is worth pointing out that the effect of this structural disorder is mainly due to the presence of vacancies at the B sites, as will be discussed below. The vacancies at A (La) sites do not produce any significant change in the magnetotransport properties.[21] Furthermore, the substitutional disorder produced by the replacement of La for Na does not seem to affect significantly the properties in these manganite series, as the sample with the highest Na substitution is the one that shows the minimum values of the resistivity, cf. Fig. 4.

The most noticeable effect of the increase in the concentration of cationic vacancies at B sites is the decrease in the critical temperature. We have previously reported how the critical temperature for ferromagnetic ordering T_c is determined by the concentration of vacancies at B sites ε, that, as stated above, is controlled by the appropriate substitution of alkaline cations in place of La^{3+} cations,[13] (note that $\varepsilon=v_B$). The correlation between T_c and ε has been explained to be a result of trapping of holes at Mn sites adjacent to the cationic vacancies, due to the modification of the periodic potential seen by the electrons. Within this framework, an increasing concentration of B cationic vacancies gives rise to a subsequent decrease in both the number of Mn ions par-

ticipating in the delocalization of carriers and the number of free holes. Consequently, the double-exchange contribution to the critical temperature for the ferro- to paramagnetic transition, according to the model of De Gennes[3] will diminish as ε increases. As a result, the magnetic and transport properties of the samples will also be significantly modified.

Two mechanisms can be invoked in order to explain the modification of the electrostatic potential seen by the charge carriers in the presence of Mn vacancies in the perovskite structure:

(i) An effective electrostatic interaction takes place between the Mn vacancies, whose effective charge is -3, and the Mn ions in its vicinity. In this situation, the Mn^{4+} ions will be more easily trapped around the *B*-position vacancies.

(ii) Also, in the Mn-O-V_{Mn} linkages the Mn-O bond length decreases. This produces an effective increase of the Mn valence; i.e., the Mn^{4+} ions will preferentially occupy these positions.[22]

As a consequence of these trapping processes the number of free holes, associated with the Mn^{4+} ions, will decrease as the concentration of vacancies is progressively higher.

B. Small-polaron transport behavior

Above the transition temperature, we have analyzed resistivity and thermopower data of our samples using a small-polaron approach.[23] Resistivity and thermopower values, in the adiabatic limit, are given, respectively, by

$$\rho(T)=\rho_0 T\exp(E_\rho/kT),$$

$$S=k/e(E_s/kT+\beta),$$

where ρ_0 is a temperature-independent factor, related to the frequency of the optical longitudinal phonons[23(f)] and β is a constant.[24] Then, resistivity and thermopower values increase upon cooling down, cf. Figs. 4 and 6, indicating a progressive localization of the charge carriers in the form of small magnetic polarons. The experimental values of E_ρ and E_S are listed in Table I. The difference between these two values, $W_H=E_\rho-E_S$, provides a measurement of the formation energy of the small polarons, which is roughly $2W_H$. In this case we have found it to be $\approx$200 meV, irrespective of the degree of disorder. The values of these energies W_H for the different samples of the series are listed in Table I.

Within this framework and related to the magnetic properties, it should be pointed out that in the temperature range of our studies a purely paramagnetic regime has not been reached ($\mu_{\rm eff}^{\rm CW}\gg\mu_{\rm eff}^{\rm th}$) at temperatures above T_c in all our samples, cf. Fig. 3. Such an experimental behavior has already been observed for related mixed-valence manganites, and it was explained in terms of the formation of small magnetic polarons above T_c.[25] Hence, according to the work of de Teresa *et al.*,[25] when cooling, the charge carriers become localized at temperatures close to 400 K, presumably due to strong electron-phonon coupling associated with the Jahn-Teller effect. This gives rise to a strong local deformation of both the nuclear lattice (as reflected by the anomalous thermal expansion at T_c-400 K temperature range) and the spin lattice. Also the magnetic moments around the charge carrier become polarized: a strong ferromagnetic correlation is observed by magnetic measurements, and small-angle neutron-scattering (SANS) experiences show the formation of ferromagnetic clusters.[25]

Except for the $x=0.00$ sample, whose special features will require us to return again to the effects associated with its high structural disorder, the behavior in the $La_{1-x}Na_xMnO_{3+\delta}$ series fits in well with this approach. Thus, when the magnetic order is achieved, a change in the thermal dependence of resistivity and thermopower is observed. Indeed, both properties reach their maximum values at temperatures slightly lower than T_c. Then, the resistivity changes from semiconducting ($\partial\rho/\partial T<0$) to metalliclike behavior ($\partial\rho/\partial T>0$), and the thermopower drops to a constant value, close to zero. The temperature and magnetic-field dependences of thermopower are indicative of a progressive release of trapped carriers as ferromagnetic order develops. These results are consistent with previous SANS experiments which showed that, when the temperature approaches T_c, and also by the application of a magnetic field, the ferromagnetic clusters grow in size and decrease in number.[25] This result suggests that the ferromagnetic order induce the delocalization of the charge carriers. The release of trapped carriers is reflected in the decrease of $\alpha(T,H)$.

Nevertheless, the particular behavior of the sample $x=0.00$, i.e., the occurrence of a magnetic transition that is not accompanied by a change in the transport character, would still remain unexplained in the context of the DE model. Thus, it seems necessary to search for a complementary approach that provides a more complete picture of this phenomenology.

C. Metal to insulator transition: effect of disorder

Traditionally two mechanisms have been invoked in order to explain the metal-to-insulator transitions in these systems. On one side, a strong coupling to the lattice can localize charge carriers as small polarons.[7] The conduction processes of these entities are explained in the framework of the Holstein model. This satisfactorily explains some properties of the manganite system, namely the isotopic effect,[15] the anomalous Hall effect,[23(d)] and the different activation energies between resistivity and thermopower.[23(c)] On the other side, it has been recently suggested that the effect of the structural disorder, which would modify the electrostatic potential seen by the charge carriers, could account for the metal-to-insulator transition.[16,26,27] In this context it seems that a strong electron-phonon coupling and a substantial amount of disorder are required to account for the insulating character of the paramagnetic phase.[8(b)]

Within these models of disorder, Sheng *et al.*[26] have concluded that there should be three possible different electronic regimes as a function of the disorder. Thus, without prejudice to the ferro- to paramagnetic transition, which would occur in all cases, (a) the system must exhibit metallic behavior in all the temperature range when the degree of disorder is small, cf. Fig. 8(a), since the Fermi level lies in the region of extended states in the whole temperature range; (b) for a high degree of disorder, the system would behave always as insulator, cf. Fig. 8(c), since the Fermi level lies in the region of localized states; and (c) for intermediate situations, a metal-to-insulator transition, intimately related to the

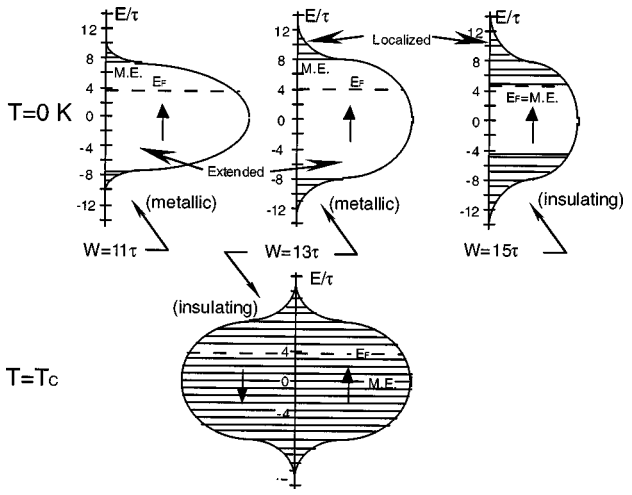

FIG. 8. Schematic representation of the electronic band diagram for different values of the disorder, both at 0 K and at $T \geqslant T_c$. The random on-site energies due to nonmagnetic disorder are distributed in the range $[-W/2,W/2]$, τ is the transfer integral, and E is the single-electron energy, eigenvalue of the Hamiltonian, according to Ref. 26. The structural disorder originates a broadening of the e_g conduction band and the appearance of localized energy levels at the bottom and top of it.

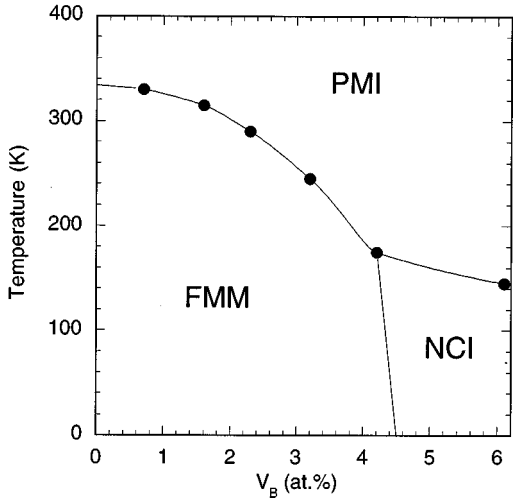

FIG. 9. Proposed phase diagram for $La_{1-x}Na_xMnO_{3+\delta}$ as a function of the concentration of vacancies at B sites, with a constant tolerance factor throughout the series. Solid circles represent the experimental values of the observed magnetic transition temperatures.

magnetic transition, is predicted, since in this case the Fermi level will cross the mobility edge as the temperature is raised, cf. Fig. 8(b). In practice, several experimental features encountered in our samples are explained within this model:

(i) An increase by several orders of magnitude in the residual resistivity $[\rho(0\ \mathrm{K})]$ with increasing disorder.
(ii) Metal-to-insulator transition temperatures that decrease with increasing disorder.
(iii) The existence of samples with higher degree of disorder that show concomitant ferromagnetism and insulatinglike conductivity.

Thus, the insulator-to-metal transition is observed for the $La_{1-x}Na_xMnO_{3+\delta}$ samples in which x varies from 0.03 ($v_B = 4.3\%$) to 0.15 ($v_B = 0.5\%$). In contrast, the $x = 0.00$ samples ($v_B = 5.1\%$) would correspond to a point in the phase diagram with higher structural disorder (see Fig. 9).

From the study of the electronic properties of a similar system, i.e., $LaMnO_{3+\delta}$ (for $\delta \leqslant 0.15$), Ritter *et al.*[14(c)] concluded that the low-temperature behavior of samples having a high structural disorder could be understood in terms of the existence of ferromagnetic clusters embedded in a matrix with a cluster-glass magnetic behavior. It seems reasonable to expect a similar explanation in the present case as well. Intuitively, at low temperatures, as a consequence of disorder in $La_{1-x}Na_xMnO_{3+\delta}$, there will coexist ferromagnetic-metallic regions (clusters), where the DE mechanism will take place, and cluster-glass semiconducting zones. As the structural disorder is introduced in the system, the total volume occupied by the semiconducting regions progressively increases. The residual resistivity of the samples will subsequently increase. The $x = 0.00$ sample in the $La_{1-x}Na_xMnO_{3+\delta}$ series represents the situation of highest disorder for which the metallic regions seem to be in the threshold of percolation. The conductivity, in this situation, will be semiconductinglike, although locally a ferromagnetic order will be still present. This seems to give rise to a noncollinear magnetic structure and to a decrease of the magnetic moment, as observed experimentally, cf. Figs. 1 and 2.

Thermopower data are consistent with the above description. As far as only metallic regions contribute to thermopower values, regardless of the volume fraction occupied by the metallic regions, ''metallic'' characteristics are expected in the Seebeck coefficient for the $x = 0.00$ sample, which seems to be the case in our present study. It is also important to recall that Zhou *et al.*[28] suggested that the existence of a new extended electronic state (resulting from the strong coupling at low temperatures between the conduction electrons and cooperative oxygen vibrations along the Mn-O bond axes) is responsible for the temperature-independent $\alpha(T) = 0$ behavior at low temperatures. Indeed, it is in this context that our above reference to ''metallic'' characteristics of the Seebeck coefficient values should be interpreted.

V. CONCLUDING REMARKS

The results of our study on manganite samples in the $La_{1-x}Na_xMnO_{3+\delta}$ series are especially appropriate because (1) The Mn^{3+}/Mn^{4+} ratio in the samples remains practically constant through the entire series; the mean oxidation state of Mn is close to 3.33, a value considered as optimum for CMR. In this way, the total concentration of holes will not change throughout the series. (2) Given that La^{3+} and Na^{+} ions have similar radii, the tolerance factor of the perovskite structure will remain practically unchanged for all the samples. Under these considerations, the systematics observed in the electronic properties of these materials must be related to the structural disorder produced by the presence of cationic vacancies at the B sites of the perovskite structure. This last variable can, in turn, be chemically controlled by the appropriate substitution of alkaline cations in place of La^{3+} cations.

As the structural disorder increases the residual resistivity

of the sample increases by eight orders of magnitude. The transition temperature from the ferromagnetic metallic phase to the paramagnetic semiconducting one decreases from 330 to 140 K. Furthermore, the sample with the highest concentration of vacancies ($x=0.00$), i.e., the highest structural disorder, remains in a semiconducting state even in the magnetically ordered phase where a noncollinear magnetic state is evidenced from magnetization measurements. Magnetization and transport measurements suggest the existence of small magnetic polarons whose formation energies are determined to be $\approx$200 meV, irrespective of the degree of disorder in the samples.

These results may be explained in the framework of the model of Sheng *et al.*,[26] assuming the coexistence of ferromagnetic and cluster glass regions below the temperature of the magnetic transition. The volume fraction occupied by the former regions will determine the transport properties of this manganite series.

Further experiences in order to determine explicitly the effect of the structural disorder on the electron-phonon coupling could shed light on the understanding of the properties of these kinds of samples.

ACKNOWLEDGMENTS

J.V., R.J.O.-H., and F.S. acknowledge many helpful discussions with Professor D. Beltrán, Professor A. M. Grishin, and Professor E. D. Dahlberg as well as with Dr. C. Gómez-Polo, Dr. J. I. Pérez de Landazábal, and Dr. V. Recarte. We greatly appreciate interactions with V. Ström and B. J. Jönsson while using the sensitive ac susceptometer designed and constructed by them. The research in Sweden was supported by the Funding Agency NUTEK. The Spanish Comisión Interministerial de Ciencia y Tecnología (CICYT, MAT96-1037) and the Generalitat Valenciana (GV-2227/94) supported the research in Valencia. Z.E.-F. is grateful to the Instituto de Cooperación con el Mundo Arabe (Agencia Española de Coopoeración Internacional, Ministerio de Asuntos Exteriores) and the Universitat de València for grants. The SCSIE of the Universitat de València is acknowledged for x-ray diffraction and analytical facilities.

*On leave from the Département de Chimie, Faculté des Sciences, Université Abdelmalek Essaadi, Tétouan, Morocco.

[1] Z. Zener, Phys. Rev. **82**, 403 (1951).

[2] P. W. Anderson, Phys. Rev. **100**, 675 (1955).

[3] P. G. de Gennes, Phys. Rev. **116**, 141 (1960).

[4] R. von Helmolt, J. Wecker, B. Holzapfel, L. Schultz, and K. Samwer, Phys. Rev. Lett. **71**, 2331 (1993).

[5] S. Jin, T. H. Teifel, M. McCormack, R. A. Fastnacht, R. Ramesh, and L. H. Chen, Science **264**, 413 (1994).

[6] A. Hellemans, Science **273**, 880 (1996).

[7] A. J. Millis, P. B. Littewood, and B. I. Sharaiman, Phys. Rev. Lett. **74**, 5144 (1995).

[8] (a) H. Röder, J. Zang, and A. R. Bishop, Phys. Rev. Lett. **76**, 1356 (1996); (b) Q. Li, J. Zhang, A. R. Bishop, and C. M. Soukoulis, Phys. Rev. B **56**, 4541 (1997).

[9] A. J. Millis, Nature (London) **392**, 147 (1998).

[10] P. Schiffer, A. P. Ramirez, W. Bao, and S. W. Cheong, Phys. Rev. Lett. **75**, 3336 (1995).

[11] (a) H. Y. Hwang, S. W. Cheong, P. G. Radaelli, M. Marezio, and B. Batlogg, Phys. Rev. Lett. **75**, 914 (1995); (b) J. Fontcuberta, B. Martinez, A. Seffar, S. Piñol, J. L. García-Muñoz, and X. Obradors, *ibid.* **76**, 1122 (1996).

[12] Y. Ng-Lee, F. Sapiña, E. Martinez-Tamayo, J. V. Folgado, R. Ibañez, D. Beltrán, F. Lloret, and A. Segura, J. Mater. Chem. **7**, 1905 (1997).

[13] T. Boix, F. Sapiña, Z. El-Fadli, E. Martinez, A. Beltrán, J. Vergara, R. J. Ortega, and K. V. Rao, Chem. Mater. **10**, 1569 (1998).

[14] (a) J. Töpfer and J. B. Goodenough, J. Solid State Chem. **130**, 117 (1997); (b) Chem. Mater. **9**, 1467 (1997); (c) C. Ritter, M. R. Ibarra, J. M. De Teresa, P. A. Algarabel, C. Marquina, J. Blasco, J. García, S. Oseroff, and S. W. Cheong, Phys. Rev. B **56**, 8902 (1997); (d) J. Töpfer, J. P. Doumerc, and J. C. Grenier, J. Mater. Chem. **6**, 1511 (1996); (e) V. Ferris, L. Brohan, M. Ganne, and M. Tournoux, Eur. J. Solid State Inorg. Chem. **32**, 131 (1995); (f) V. Ferris, G. Goglio, L. Brohan, O. Joubert, P. Molinié, P. Dordorand, and M. Ganne, Mater. Res. Bull. **32**, 763 (1997); (g) G. Goglio, A. Maignan, V. Ferris, L. Brohan, and M. Ganne (unpublished); (h) A. Arulraj, R. Mahesh, G. N. Subbanna, R. Mahendiran, A. K. Raychaudhuri, and C. N. R. Rao, J. Solid State Chem. **127**, 87 (1996); (i) A. Gupta, T. R. McGuire, P. R. Duncombe, M. Rupp, J. Z. Sun, W. J. Gallagher, and G. Xiao, Appl. Phys. Lett. **67**, 3494 (1995); (j) J. A. Alonso, M. J. Martinez-Lope, M. T. Casais, J. L. MacManus-Driscoll, P. S. de Silva, L. F. Cohen, and M. T. Fernandez-Diaz, J. Mater. Chem. **7**, 2139 (1997); (k) B. Raveau, A. Maignan, C. Martin, and M. Hervieu, Chem. Mater. **19**, 2641 (1998); (l) F. Damay, C. Martin, A. Maignan, and B. Raveau, J. Magn. Magn. Mater. **183**, 143 (1998); (m) A. Maignan, C. Michel, M. Hervieu, and B. Raveau, Solid State Commun. **101**, 277 (1997); (n) R. Mahendiran, S. K. Tiwary, A. K. Raychaudhuri, T. V. Ramakrishnan, R. Mahesh, N. Rangavittal, and C. N. R. Rao, Phys. Rev. B **53**, 3348 (1996).

[15] G. Zhao, K. Conder, H. Keller, and K. A. Müller, Nature (London) **381**, 676 (1996).

[16] L. Sheng, D. Y. Xing, D. N. Sheng, and C. S. Ting, Phys. Rev. Lett. **79**, 1710 (1997).

[17] H. Y. Hwang, S. W. Cheong, N. P. Ong, and B. Batlogg, Phys. Rev. Lett. **77**, 2041 (1996).

[18] P. Mandal, K. Barner, L. Haupt, A. Poddar, R. von Helmolt, A. G. M. Jansen, and P. Wyder, Phys. Rev. B **57**, 10 256 (1998).

[19] J. B. Goodenough, J. Appl. Phys. **81**, 5330 (1997).

[20] I. G. Krogh Andersen, E. Krogh Andersen, P. Norby, and E. S. Kou, J. Solid State Chem. **113**, 320 (1994).

[21] S. V. Pietambaram, D. Kumar, R. K. Singh, and C. B. Lee, Phys. Rev. B **58**, 8182 (1998).

[22] I. D. Brown, *Structure and Bonding in Crystals* (Academic, New York, 1981), Vol. II, p. 1.

[23] (a) J. Tanaka, S. Ehara, S. Tamura, M. Tsukioka, and M. Umehara, J. Phys. Soc. Jpn. **51**, 1236 (1982); (b) M. Jaime, M. B. Salamon, K. Pettit, M. Rubinstein, R. E. Treece, J. S. Horwitz, and D. B. Chrisey, Appl. Phys. Lett. **68**, 1576 (1996); (c) M. Jaime, M. B. Salamon, M. Rubinstein, R. E. Treece, J. S. Horwitz, and D. B. Chrisey, Phys. Rev. B **54**, 11 914 (1996); (d) M. Jaime, H. T. Hardner, M. B. Salamon, M. Rubinstein, P. Dorsey, and D. Emin, Phys. Rev. Lett. **78**, 951 (1997); (e) D. C. Worledge, L. Miéville, and T. H. Geballe, Phys. Rev. B **57**, 15 267 (1998); (f) M. Ziese and C. Srinitiwarawong, *ibid.* **58**, 11 519 (1998).

[24] (a) M. F. Hundley and J. J. Neumeier, Phys. Rev. B **55**, 11 511 (1997); (b) J. Hejtmanek, Z. Jirak, K. Sedmidubsky, A. Maignan, Ch. Simon, V. Caignaert, C. Martin, and B. Raveau, *ibid.* **54**, 11 947 (1996).

[25] J. M. De Teresa, M. R. Ibarra, P. A. Algarabel, C. Ritter, C. Marquina, J. Blasco, J. García, A. Del Moral, and Z. Arnold, Nature (London) **386**, 256 (1997).

[26] L. Sheng, D. Y. Xing, D. N. Sheng, and C. S. Ting, Phys. Rev. B **56**, 7053 (1997).

[27] R. Allub and B. Alascio, Phys. Rev. B **55**, 14 113 (1997).

[28] J. S. Zhou, W. Archibald, and J. B. Goodenough, Nature (London) **381**, 770 (1996).